Steel and Composite Structures, *Vol. 36, No. 3* (*2020*) *293-305*
DOI: https://doi.org/10.12989/scs.2020.36.3.293

Dynamic analysis of functionally graded nonlocal nanobeam with different porosity models

Emad E. Ghandourah*[1] and Azza M. Abdraboh[2a]

[1]*Nuclear Engineering Dept., Faculty of Engineering, King Abdulaziz University, P.O. Box 80204, Jeddah 21589, Saudi Arabia*
[2]*Physics Department, Faculty of Science, Banha University, Banha, Egypt*

(*Received April 30, 2020, Revised July 6, 2020, Accepted July 7, 2020*)

Abstract. This article presented a nanoscale modified continuum model to investigate the free vibration of functionally graded (FG) porous nanobeam by using finite element method. The main novelty of this manuscript is presenting effects of four different porosity models on vibration behaviors of nonlocal nanobeam structure including size effect, that not be discussed before The proposed porosity models are, uniform porosity distribution, symmetric with mid-plane, bottom surface distribution and top surface distribution. The nano-scale effect is included in modified model by using the differential nonlocal continuum theory of Eringen that adding the length scale into the constitutive equations as a material parameter constant. The graded material is distributed through the beam thickness by a generalized power law function. The beam is simply supported, and it is assumed to be thin. Therefore, the kinematic assumptions of Euler-Bernoulli beam theory are held. The mathematical model is solved numerically using the finite element method. Results demonstrate effects of porosity type, material gradation, and nanoscale parameters on the free vibration of nanobeam. The proposed model is effective in vibration analysis of NEMS structure manufactured by porous functionally graded materials.

Keywords: free vibration; functionally graded nanobeam; porosity models; nonlocal elasticity theory; finite element method

1. Introduction

New innovative composite materials, known as Functionally graded materials (FGMs), were proposed firstly in Sendai area for addressing heat-resistant problem by Japanese scientists in 1984 during the space-plane project, (Alshorbagy *et al.* 2011, Miyamoto *et al.* 2013). FGMs offer smooth and continuous distribution of two or more materials along one or more directions by a specific function. FGMs have potential applications in various fields such as aircraft, space vehicles, rocket engine, automotive industries, optics, barrier coating, nuclear reactors, Hamed *et al.* (2016), and in nano-structures application such as micro-/nano-electro-mechanical-systems (MEMS/NEMS), thin films, shape memory alloys, and atomic force microscopes (AFM), Eltaher *et al.* (2012).

To investigate mechanical response of nanostructure accurately, modified continuum model theories such as, nonlocal of elasticity of Eringen [Eltaher *et al.* (2016a, b, c), Phung-Van *et al.* (2017a, 2018), Eltaher *et al.* (2019a), Eltaher and Mohamed (2020a), Fenjan *et al.* (2020)], couple stress theory Nguyen *et al.* (2017), Thanh *et al.* (2018), Akbas (2018a), Thanh *et al.* (2019a, b, c), Akbas (2019b), Surface elasticity theory Khater *et al.* (2014), Agwa and Eltaher (2016), Almitani (2020), energy equivalent method of CNTs Eltaher and Agwa (2016), Eltaher *et al.* (2019b), Mohamed *et al.* (2020), and doublet mechanic Gul and Aydogdu (2018) and Mohamed *et al.* (2020), Eltaher and Mohamed (2020a) are exploited to include the size-scale effects.

Since, the size-scale effect is missing in classical continuum mechanics, nonlocal theories of continuum mechanics are widely used in order to assess size effects in nanostructures, Apuzzo *et al.* (2017). Reddy (2007) and Thai (2012) presented analytical solutions for mechanical behaviors of nonlocal nanobeam included higher order beam theories. Reddy (2011) developed microstructure-dependent nonlinear Euler–Bernoulli and Timoshenko FG beam theories to study the size effect on postbuckling of nanobeam. Eltaher *et al.* (2012, 2013a) studied bending, buckling and free vibration of FG nonlocal nanobeam by using finite element method. Simsek and Yurtcu (2013) presented an analytical solution for bending and buckling of FG nanobeams based on the nonlocal Timoshenko beam theory. Eltaher *et al.* (2013b, 2014a, b) presented effect of neutral axis position natural frequencies of FG macro/nanobeams included a nonlocal elasticity for Euler and Timoshenko beam theories. Shaat *et al.* (2013) studied nonlinear size-dependent FE of FG tiny-bodies considering surface energy effects. Rahmani and Pedram (2014) analyzed and modeled the size effect on vibration of FG nonlocal Timoshenko nanobeams. Eltaher *et al.* (2016) presented a comprehensive review on the importance of nonlocal elasticity in analysis of mechanical behaviors of nanobeam. Simsek (2016) studied nonlinear free vibration

*Corresponding author, Associate Professor
E-mail: eghandourah@kau.edu.sa
[a]Ph.D.
E-mail: aza.abdrabo@fsc.bu.edu.eg

http://www.techno-press.org/?journal=scs&subpage=8
ISSN: 1229-9367 (Print), 1598-6233 (Online)

of FG nanobeam using nonlocal strain gradient theory via Hamiltonian approach. Hamed *et al.* (2016) studied free vibration of symmetric and sigmoid FG nonlocal nanobeams by using finite element method. Ahouel *et al.* (2016) investigated bending, buckling, and vibration of FG nanobeams using the nonlocal differential constitutive relations of Eringen. Akbas (2017a) explored forced vibration responses of FG modified couple stress theory nanobeams with damping effect excited by a transverse triangular impulse force. Apuzzo *et al.* (2017) studied free vibrations of Bernoulli-Euler nano-beams by using the stress-driven nonlocal integral model. Trabelssi *et al.* (2017) examined free vibration response of a nonlocal nonlinear FG Euler–Bernoulli nanobeam resting on a nonlinear elastic foundation. Emam *et al.* (2018) explored postbuckling and free vibration of multilayer imperfect nanobeams under a pre-stress load. Barretta *et al.* (2018) developed exact solutions of inflected FG nano-beams modeled by integral elasticity theory. Soliman *et al.* (2018) and Eltaher *et al.* (2018a) investigated the dynamic transient response of FG pipe subjected to internal pressure and unsteady temperature. Heydari (2018) analyzed vibration and buckling of arbitrary gradation of nano-higher order rectangular beam. Mirzaei *et al.* (2019) exploited first-order shear deformation theory to study time-dependent creep of FG beam with trapezoidal cross section. Rahmani *et al.* (2018) studied free vibration of deep curved FG nano-beam based on modified couple stress theory. Liu *et al.* (2019) examined the nonlinear vibrational behaviors of FG sandwich nonlocal strain gradient nanobeams in the presence of initial geometric imperfection. Bambaeechee (2019) developed exact analytical solutions for the free vibration of AFG and uniform beams with general elastic supports by using Euler-Bernoulli beam theory. Simsek (2019) derived closed-form solutions for static, buckling, free and forced vibration of FG nanobeams using nonlocal strain gradient theory. Aria and Friswell (2019) developed a nonlocal finite element model to study buckling and vibration of FG nanobeams. Melaibari *et al.* (2020) investigated static stability of higher order FG beam under variable axial load. Hamed *et al.* (2020a) studied buckling analysis of sandwich beam rested on elastic foundation and subjected to varying axial in-plane loads. Karami *et al.* (2020) explored dynamic behavior of two-dimensional FG tapered Timoshenko nanobeam in thermal environment using nonlocal strain gradient theory. Akbas *et al.* (2020) and Asiri *et al.* (2020) studied dynamic response of layered FG viscoelastic deep beams under pulse load by using finite element method.

FGMs can be manufactured by self-propagating high temperature synthesis, multi-step sequential infiltration technique, and non-pressure sintering technique. In these processes, porosities and micro-voids may occur inside materials owing to the technical issues, Wang *et al.* (2017), Lee and Ahn (2018) and Matuła *et al.* (2019). The porosity and voids can weaken the strength of FGMs dramatically and adverse effects on required properties of structures.

Porous FG materials are found naturally around us, such as, bamboo with density gradients along the radial direction in its cross section, human cancellous bone which is sponge-like cellular structure, banana peel, and elk antler, etc. Artificial FGPMs, such as biomedical implants, cushioning materials, filtration materials and drug delivery devices, Zhang and Wang (2017). Various techniques, such as, Gas foaming, phase separation techniques, solvent casting and particle leaching, selective laser sintering, stereolithography, and fused deposition modeling have been used to manufacture porous materials, Zhang and Wang (2017). Recently, representative porous materials extensively used in lightweight structures, aerospace and automotive industries, due to their outstanding multi-functionality obtained by low specific weight, efficient capacity of energy dissipation, reduced thermal and electrical conductivity, Kitipornchai *et al.* (2017).

Yahia *et al.* (2015) presented analytic dispersion relation for wave propagation in FG higher-order plates with porosities. Akbas (2015) investigated free vibration and bending of FG beams resting on elastic foundation. Galeban *et al.* (2016) studied free vibration of FG thin beams made of saturated porous materials. Ebrahimi and Habibi (2016) analyzed deflection and vibration of higher-order shear deformable compositionally graded porous plate. Amar *et al.* (2017) presented effects of power-law exponents, porosity distributions, porosity volume fractions, the material length scale parameter and slenderness ratios on bending and dynamic responses of FG micro-beam modeled by modified couple stress theory (MCST). Akbas (2017b, c, d) investigated the free vibration and bending behavior of temperature-dependent FG porous deep beams with different porosity models under mechanical and thermal loads. Mirjavadi *et al.* (2017) studied the effect of thermal on vibration of two-dimensional FG porous Timoshenko nanobeams. Jandaghian and Rahmani (2017) investigated vibration of FG nanobeams based on third-order shear deformation theory under various boundary conditions. Phung-Van *et al.* (2017b) studied nonlinear transient isogeometric analysis of smart piezoelectric functionally graded material plates based on generalized shear deformation theory under thermo-electro-mechanical loads. Akbas (2018b) examined numerically effects of material distribution, porosity coefficients, nonlinear effects on the static behavior of FG beams. Akbas (2018c) investigated forced vibration analysis of FG porous deep plane stress beams under dynamically load. Yousfi *et al.* (2018) developed an analytical solution of the Navier type for free vibration analysis of FG porous plate. Guessas *et al.* (2018) investigated analytically the effect of porosity on the buckling behavior of carbon nanotube-reinforced composite porous. Nguyen *et al.* (2018) studied free vibration of tapered BFGM beams using an efficient shear deformable finite element model. Eltaher *et al.* (2018b) proposed modified porosity model to study free vibration of FG porous nanobeams. Benahmed *et al.* (2019) studied critical buckling of FG nanoscale beam with porosities by using nonlocal higher-order shear deformation. Hamed *et al.* (2019) examined effects of porosity models on static behavior of size dependent FG nanobeam by using nonlocal elasticity theory. Khatir *et al.* (2019) exploited Artificial Neural Network (ANN) combined with Particle Swarm Optimization (PSO) for damage quantification in laminated composite plates using Cornwell indicator (CI). Mekerbi *et al.* (2019) analyzed thermal buckling of FG plates with porosity and resting on elastic foundation by using quasi 3D theory. Thanh *et al.* (2019d) presented the size-dependent effects on thermal buckling and post-buckling behaviors of FG material micro-plates with porosities by using isogeometric analysis. Yuksel and Akbas (2019) presented buckling analysis of fiber-reinforced laminated composite plate with porosity effects within the first shear deformation plate theory. Akbas (2019b) presented forced vibration analysis of sandwich deep beams made of FGM in face layers and a porous material in core layer. Akbas (2019c) studied hygro-thermal post-buckling analysis of a FG beam by using Newton-Raphson method and finite element method. Berghouti *et al.* (2019) presented vibration analysis of nonlocal porous nanobeams made of functionally graded material. Phung-Van *et al.* (2019) presented the influence of porosity on nonlinear transient responses of functionally graded nanoplates by using isogeometric analysis. Hamed *et al.* (2020b) studied influence of axial load function and optimization on static stability of sandwich FG beams with porous core. Gafour *et al.* (2020) exploited non-local shear deformation and energy principle to study free vibration of FG porous nanobeam. Eltaher and Mohamed (2020c) studied buckling of FG beam under variable axial in-plane load by using differential quadrature method. Zhao *et al.* (2020) presented effects of porosity and flexoelectricity on static bending and free vibration of FG piezoelectric nanobeams.

As predicated from literature, the dynamic free vibration behavior of FG nonlocal nanobeam with different porosity models by suing finite element method has not been addressed. So, this paper presented a numerical model to present effects of uniform, symmetric, bottom surface top surface porosity models on the natural frequencies of FG nanobeam. Nonlocal differential form of Eringen is exploited to include the size-scale effect in modified continuum model. The following sections of a manuscript are arranged as: Section 2 depicts constitutive material equations, porosity models, kinematic relation, nonlocal elasticity and mathematical equation of motion. Section 3 is devoted to the numerical finite element method and element matrices. Numerical results and parametric studies of porosity models, material gradation parameter, and nanoscale effect on the first five natural frequencies of nanobeam are discussed through Section 4. Conclusion and main points of the present study is summarized in Section 5.

2. Mathematical formulation

2.1 Material graduation functions

The gradation of function graded material can be presented and modeled by a simple homogenization Voigt rule, Hamed *et al*. (2016). The volume fraction of materials are graded across the beam thickness (z) by the following functions, Alshorbagy *et al*. (2011)

$$V_c = \left(\frac{1}{2} + \frac{z}{h}\right)^n \qquad \& \qquad V_m = 1 - \left(\frac{1}{2} + \frac{z}{h}\right)^k \qquad (0 \leq n < \infty) \tag{1}$$

where V, k , h are volume fraction, gradation parameter, and beam thickness, respectively. subscripts c and m represent ceramic and metal materials, respectively. Therefore, the gradation of Young's modulus (E) and density (ρ) of FG materials can be depicted by a generalized power law function as

$$E(z) = (E_c - E_m)\left[\frac{1}{2} + \frac{z}{h}\right]^k + E_m$$
$$\rho(z) = (\rho_c - \rho_m)\left[\frac{1}{2} + \frac{z}{h}\right]^k + \rho_m \tag{2}$$

2.2 Porosity models

It is observed from experimental examination that linear variation of porosity is inadequate to consider a reduction in the rigidity of a structure. Thus, four porosity models are proposed through this study. The first model is proposed by Wattanasakulpong and Ungbhakorn (2014), presumed that the porosity is uniformly distributed through the thickness of the beam by the following [Model 1], as shown in Fig. 1

$$E(z) = [E_c - E_m]\left(\frac{1}{2} + \frac{z}{h}\right)^k + E_m - \frac{\alpha}{2}\ [E_c + E_m] \tag{3a}$$

$$\rho(z) = [\rho_c - \rho_m]\left(\frac{1}{2} + \frac{z}{h}\right)^k + \rho_m - \frac{\alpha}{2}\ [\rho_c + \rho_m] \tag{3b}$$

In which α is the volume fraction of porosity in the material. The last term of the equation represents the porosity content in both metal and ceramic constituents.

The model 2 of the porosity, assumed that the porosity is distributed symmetric around mid-axis and its peak lies near to mid-axis and decreased continuously as moved away to top or bottom surface. The material distributions for a symmetric model, shown in Fig. 2, can be implemented by

$$E(z) = \left\{[E_c - E_m]\left(\frac{1}{2} + \frac{z}{h}\right)^k + E_m\right\}\left\{1 - \alpha\ \cos\left[\pi\left(\frac{z}{h}\right)\right]\right\} \tag{4a}$$

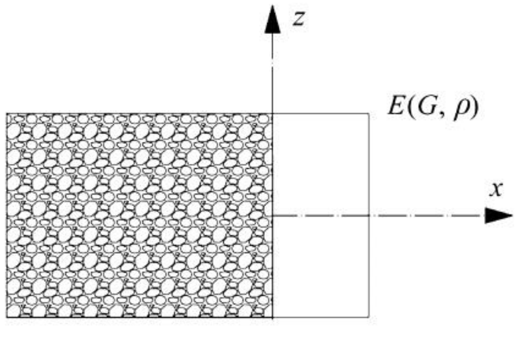

Fig. 1 Uniform porosity distribution Model 1, Thang *et al.* (2018)

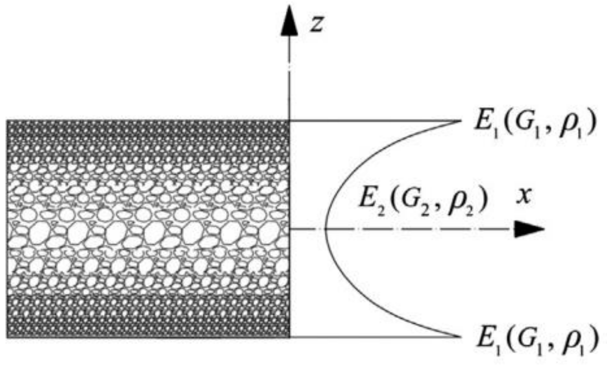

Fig. 2 Symmetric porosity distribution Model 2, Thang *et al.* (2018)

$$\rho(z) = \left[[\rho_c - \rho_m] \left(\frac{1}{2} + \frac{z}{h} \right)^k + \rho_m \right] \left[1 - \alpha \ \cos\left[\pi \left(\frac{z}{h} \right) \right] \right] \quad (4b)$$

The third model assumed that the porosity is concentrated at the bottom surface and decreases upwards, as shown in Fig.3. Hence, the porous material gradated through the thickness by the following

$$E(z) = \left[[E_c - E_m] \left(\frac{1}{2} + \frac{z}{h} \right)^k + E_m \right] \left[1 - \alpha \ \cos\left[\frac{\pi}{2} \left(\frac{z}{h} + \frac{1}{2} \right) \right] \right] \quad (5a)$$

$$\rho(z) = \left[[\rho_c - \rho_m] \left(\frac{1}{2} + \frac{z}{h} \right)^k + \rho_m \right] \left[1 - \alpha \ \cos\left[\frac{\pi}{2} \left(\frac{z}{h} + \frac{1}{2} \right) \right] \right] \quad (5b)$$

The fourth porosity model assumed that, the porosity is concentrated at the top surface and decreased gradually in nonlinear behavior. The fourth model can be depicted by

$$E(z) = \left[[E_c - E_m] \left(\frac{1}{2} + \frac{z}{h} \right)^k + E_m \right] \left[1 - \alpha \ \cos\left[\frac{\pi}{2} \left(\frac{z}{h} - \frac{1}{2} \right) \right] \right] \quad (6a)$$

$$\rho(z) = \left[[\rho_c - \rho_m] \left(\frac{1}{2} + \frac{z}{h} \right)^k + \rho_m \right] \left[1 - \alpha \ \cos\left[\frac{\pi}{2} \left(\frac{z}{h} - \frac{1}{2} \right) \right] \right] \quad (6b)$$

2.3 Nonlocal differential constitutive equations

Nonlocal elasticity assumed that the stress at a specified point is a functional of strain field around this point with a certain distance. The integral nonlocal equation can be portrayed as, Eltaher *et al.* (2018c, d)

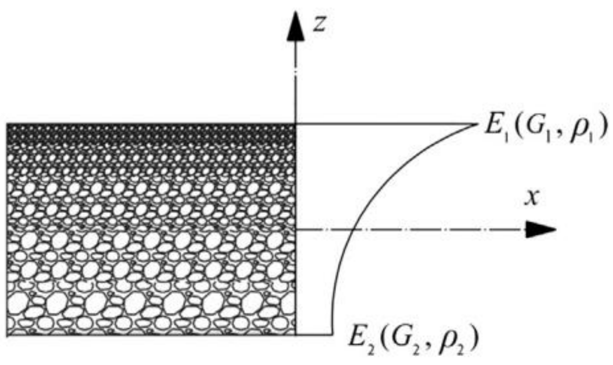

Fig. 3 Decreasing of porosity distribution upwards Model 3, Thang *et al.* (2018)

$$\sigma_{ij}(x) = \int_V \alpha(|x' - x|, \tau) \mathrm{T}_{ij}(x') \mathrm{d}x' \quad (7)$$

In which $\mathrm{T}_{ij}(x')$ are the macroscopic stress tensor at point x and $\alpha(|x' - x|, \tau)$ is nonlocal modulus function that represents the effect of interatomic bonding. τ isa material length scale constant. The macroscopic stress tensor can be described as a function of material elasticity tensor (C) and strain (ε) by generalized Hooke's law as

$$\mathrm{t}(x) = C(x) \colon \varepsilon(x) \quad (8)$$

In (1983) Eringen proved that when nonlocal modulus described by a Green's function, the nonlocal constitutive relation can be reduced to the differential form as

$$[1 - (e_0 a)^2 \ \nabla^2] \sigma_{ij} = t_{ij} \quad (9)$$

wheree_0 is a constant to match the reliable results by experiments,a is the internallength scale, and ∇^2 is the Laplacian operator. For one-dimensional nonlocal nanobeam, nonlocal constitute relation Eq. (9) can be written as, Eltaher *et al.* (2018 c, d)

$$\sigma_{xx} - \mu \frac{\partial^2 \sigma_{xx}}{\partial x^2} = E \varepsilon_{xx}; \quad [\mu = (e_0 a)^2] \quad (10)$$

2.4 Governing equation of motion

Based on the Euler-Bernoulli theory, where plane sections perpendicular to the neutral axis of the beam before deformation remain plane and rigid, and rotate such that they remain perpendicular to the neutral axis after deformation. The displacement field can be assumed as

$$u(x, z) = u_0(x) - z \frac{dw_0(x)}{dx} \quad (11a)$$

$$w(x, z) = w_0(x) \quad (11b)$$

where u and w are the total displacements along the coordinate (x), and u_0 and w_0 denote the axial and transverse displacements of a point on the neutral axis. According to Euler theory, the only nonzero strain is

$$\varepsilon_{xx}(x, z) = \frac{d}{dx} \left[u_0(x) - z \frac{dw_0(x)}{dx} \right] = \frac{du_0(x)}{dx} - z \frac{d^2 w_0(x)}{dx^2} = \varepsilon_{xx}^0 + z \varepsilon_{xx}^1 \quad (12)$$

The *nonzero classical stress* can be presented by

$$\sigma_{xx}(x, z) = E(z) \varepsilon_{xx}(x, z) = E(z) [\varepsilon_{xx}^0 + z \varepsilon_{xx}^1] \quad (13)$$

The *Axial and bending moment* can be written as

$$N_{xx} = \int_A \sigma_{xx} dA = A_{11} \varepsilon_{xx}^0 + B_{11} \varepsilon_{xx}^1 \quad (14a)$$

$$M_{xx} = \int_A z\sigma_{xx} dA = B_{11}\varepsilon_{xx}^0 + D_{11}\varepsilon_{xx}^1 \tag{14b}$$

Where

$$\begin{aligned}[A_{11}, B_{11}, D_{11}] &= b\int_h E(z)\ [1, z,\ z^2]dz \\ &= b\ \int_{-\frac{h}{2}}^{\frac{h}{2}} E_1(z)\ [1, z,\ z^2]dz\end{aligned} \tag{15}$$

and the nonlocal axial force and bending moment can be derived from Eq. (10) by product it by 1 and z then integrate over cross sectional area, results

$$N - \mu\frac{\partial^2 N}{\partial x^2} = A_{11}\varepsilon_{xx}^0 + B_{11}\varepsilon_{xx}^1 \tag{16a}$$

$$M - \mu\frac{\partial^2 M}{\partial x^2} = B_{11}\varepsilon_{xx}^0 + D_{11}\varepsilon_{xx}^1 \tag{16b}$$

Using Hamilton's principle, the equation of motion of a FG porous nonlocal nanobeam can be derived as follows

$$A_{11}\frac{\partial^2 u_0}{\partial x^2} + B_{11}\frac{\partial^3 w_o}{\partial x^3} + \left(1 - \mu\frac{\partial^2}{\partial x^2}\right)f = I_0\frac{\partial^2 u_0}{\partial t^2} - I_1\frac{\partial^3 w_0}{\partial t^2\partial x} - \mu\left[\ I_0\frac{\partial^4 u_0}{\partial t^2\partial x^2} - I_1\frac{\partial^5 w_0}{\partial t^2\partial x^3}\right] \tag{17a}$$

$$B_{11}\left(\frac{d^3 u_0}{dx^3}\right) + D_{11}\frac{d^4 w_0}{dx^4} + \left(1 - \mu\frac{\partial^2}{\partial x^2}\right)q + \left(1 - \mu\frac{\partial^2}{\partial x^2}\right)\left(\bar{N}\frac{\partial^2 w_0}{\partial x^2}\right) = \left(1 - \mu\frac{\partial^2}{\partial x^2}\right)\left[I_0\frac{\partial^2 w_0}{\partial t^2} + I_1\frac{\partial^3 u_0}{\partial t^2\partial x} - I_2\frac{\partial^4 w_0}{\partial t^2\partial x^2}\right] \tag{17b}$$

where f is the axial distributed force in x-direction, q is the transverse distributed force in z-direction, and $\bar{N}$ is the axial compressive load applied at the neutral axis and normal to the cross section. Inertia terms $I_0, I_1,$ and I_2 are described by

$$[I_0, I_1, I_2] = b\int_h \rho(z)\ [1, z,\ z^2]dz \tag{18}$$

3. Numerical formulation

The displacement components at the mid-plane (that is coincident with neutral plane in the current material distributions) of a beam element can be described as, Eltaher et al. (2013)

In-plane displacement u_0

$$u_0^{(e)}(x,t) = \sum_{i=1}^{2} N_i U_i(t) = N_1 U_1(t) + N_2 U_2(t) \quad \text{where} \quad i = 1,2 \tag{19a}$$

Transverse displacement w_o

$$\begin{aligned}\mathrm{w}_0^{(\mathrm{e})}(\mathrm{x},\mathrm{t}) &= \sum_{\mathrm{k}=1}^{4}\widetilde{\mathrm{N}}_{\mathrm{k}}\widetilde{\mathrm{W}}_{\mathrm{k}} \\ &= \widetilde{\mathrm{N}}_1 W_1 + \widetilde{\mathrm{N}}_2\theta_1 + \widetilde{\mathrm{N}}_3 W_2 + \widetilde{\mathrm{N}}_4\theta_2\end{aligned} \tag{19b}$$

where U, W and θ are the nodal displacements and slope, respectively. N_i is the Lagrangian interpolation function for in plane displacement, and $\widetilde{N}_{\mathrm{k}}$ is Hermetian interpolation shape function for transverse displacements. The variational form of the nonlocal Euler-Bernoulli beam is

$$\begin{aligned}&\int_0^T\int_0^L\Bigg\{\Bigg(\left[-\int_{-\frac{h}{2}}^{0}E_1(z)dz - \int_0^{\frac{h}{2}}E_2(z)dz\right]\frac{\partial u_0}{\partial x}\frac{\partial\delta u_0}{\partial x} + \\ &\left[\int_{-\frac{h}{2}}^{0}zE_1(z)dz + \int_0^{\frac{h}{2}}zE_2(z)dz\right]\frac{\partial^2 w_o}{\partial x^2}\frac{\partial\delta u_0}{\partial x} + \\ &\left[\int_{-\frac{h}{2}}^{0}zE_1(z)dz + \int_0^{\frac{h}{2}}zE_2(z)dz\right]\frac{\partial u_0}{\partial x}\frac{\partial^2\delta w_0}{\partial x^2} + \\ &\left[-\int_{-\frac{h}{2}}^{0}z^2E_1(z)dz - -\int_0^{\frac{h}{2}}z^2E_2(z)dz\right]\frac{\partial^2 w_0}{\partial x^2}\frac{\partial^2\delta w_0}{\partial x^2}\Bigg) + \\ &\left(f\delta u_0 + \mu\frac{\partial f}{\partial x}\frac{\partial\delta u_0}{\partial x}\right) + \left(q\delta w_0 - \mu q\frac{\partial^2\delta w_0}{\partial x^2}\right) + \\ &\left(\bar{N}\frac{\partial w_0}{\partial x}\frac{\partial\delta w_0}{\partial x} - \mu\bar{N}\frac{\partial^2 w_0}{\partial x^2}\frac{\partial^2\delta w_0}{\partial x^2}\right) + \Bigg(I_0\frac{\partial u_0}{\partial t}\frac{\partial\delta u_0}{\partial t} - \\ &\mu I_0\frac{\partial^3 u_0}{\partial t^2\partial x}\frac{\partial\delta u_0}{\partial x}\Bigg) + \Bigg(I_0\frac{\partial w_0}{\partial t}\frac{\partial\delta w_0}{\partial t} + \mu I_0\frac{\partial^2 w_0}{\partial t^2}\frac{\partial^2\delta w_0}{\partial x^2} + \\ &I_2\frac{\partial^2 w_0}{\partial t\partial x}\frac{\partial^2\delta w_0}{\partial t\partial x} - \mu I_2\frac{\partial^4 w_0}{\partial t^2\partial x^2}\frac{\partial^2\delta w_0}{\partial x^2}\Bigg) + \Bigg(I_1\frac{\partial^2 u_0}{\partial t\partial x}\frac{\partial\delta w_0}{\partial t} + \\ &\mu I_1\frac{\partial^3 u_0}{\partial t^2\partial x}\frac{\partial^2\delta w_0}{\partial x^2} - I_1\frac{\partial^2 w_0}{\partial t\partial x}\frac{\partial\delta u_0}{\partial t} + \\ &I_1\mu\frac{\partial^4 w_0}{\partial t^2\partial x^2}\frac{\partial\delta u_0}{\partial x}\Bigg)\Bigg\}dxdt \ + \int_0^t\Bigg[\bar{N}_B\ \delta u_0 + \bar{V}_B\ \delta w_0 + \\ &\bar{M}_B\ \frac{\partial\delta w_0}{\partial x}\Bigg]_0^L dt = 0\end{aligned} \tag{20}$$

By substituting Eqs. (19) into Eq. (20) and integrating over the domain, the equation of motion is derived as

$$(\mathrm{M}_l + \mu\mathrm{M}_{nl})\ \ddot{Y} + K_s\ Y + K_G\mathrm{Y} = F + Q \tag{21}$$

where M_l and M_{nl} are local and nonlocal mass matrices, respectively. K_s is the stiffness matrix of the FG beam, K_G is the geometrical stiffness matrix, Y is the generalized displacement vector, F and Q are the distributed force vector and the concentrated force vector, respectively. The element matrices and force vectors are described as follows:

The mass matrices are represented by

$$M_l = \int_0^l I_0 N_i N_j\ \ dx + \int_0^l\left(I_0\widetilde{\mathrm{N}}_{\mathrm{k}}\widetilde{\mathrm{N}}_{\mathrm{l}} + I_2\frac{\partial\widetilde{\mathrm{N}}_{\mathrm{k}}}{\partial x}\frac{\partial\widetilde{\mathrm{N}}_{\mathrm{l}}}{\partial x}\right)\ dx + \int_0^l\left(I_1\frac{\partial N_i}{\partial x}\widetilde{\mathrm{N}}_{\mathrm{l}} + I_1\frac{\partial^2\widetilde{\mathrm{N}}_{\mathrm{l}}}{\partial x^2}N_i\right)\ dx \tag{22a}$$

$$M_{nl} = -\int_0^l I_0\frac{\partial N_i}{\partial x}\frac{\partial N_j}{\partial x}\ \ dx + \int_0^l\left(I_0\widetilde{\mathrm{N}}_{\mathrm{k}}\frac{\partial^2\widetilde{\mathrm{N}}_{\mathrm{l}}}{\partial x^2} - I_2\frac{\partial^2\widetilde{\mathrm{N}}_{\mathrm{k}}}{\partial x^2}\frac{\partial^2\widetilde{\mathrm{N}}_{\mathrm{l}}}{\partial x^2}\right)\ dx + \int_0^l\left(I_1\frac{\partial N_i}{\partial x}\frac{\partial^2\widetilde{\mathrm{N}}_{\mathrm{l}}}{\partial x^2} + I_1\frac{\partial^2\widetilde{\mathrm{N}}_{\mathrm{l}}}{\partial x^2}\frac{\partial N_i}{\partial x}\right)\ dx \tag{22b}$$

The element stiffness matrix can be calculated by

$$K_u = \int_0^l\left[-\int_{-\frac{h}{2}}^{0}E_1(z)dz - \int_0^{\frac{h}{2}}E_2(z)dz\right]\frac{\partial N_i}{\partial x}\frac{\partial N_j}{\partial x}dx \quad \text{where} \quad i \text{ and } j = 1,2 \tag{22c}$$

$$K_w = \int_0^l\left[-\int_{-\frac{h}{2}}^{0}z^2E_1(z)dz - \int_0^{\frac{h}{2}}z^2E_2(z)dz\right]\frac{\partial\widetilde{\mathrm{N}}_{\mathrm{k}}}{\partial x}\frac{\partial\widetilde{\mathrm{N}}_{\mathrm{l}}}{\partial x}dx \tag{22d}$$

where k and l =1,2,3,4

$$K_{uw} = \int_0^l \left[\int_{-\frac{h}{2}}^0 zE_1(z)dz + \int_0^{\frac{h}{2}} zE_2(z)dz\right] \frac{\partial^2 \tilde{N}_k}{\partial x^2}\frac{\partial N_i}{\partial x} dx + \int_0^l \left[\int_{-\frac{h}{2}}^0 zE_1(z)dz + \int_0^{\frac{h}{2}} zE_2(z)dz\right] \frac{\partial N_i}{\partial x}\frac{\partial^2 \tilde{N}_k}{\partial x^2} d \quad (22e)$$

$$K_s = K_u + K_w + +K_{uw} \quad (22f)$$

The element geometrical stiffness matrix is represented by

$$K_G = \int_0^L \left[-\bar{N}\frac{\partial \tilde{N}_k}{\partial x}\frac{\partial \tilde{N}_l}{\partial x} + \mu\ \bar{N}\frac{\partial^2 \tilde{N}_k}{\partial x^2}\frac{\partial^2 \tilde{N}_l}{\partial x^2}\right] dx \quad (22g)$$

The force vector is given by

$$F = q\int_0^L \left[\tilde{N}_k - \mu\frac{\partial^2 \tilde{N}_k}{\partial x^2}\right]\ dx + \int_0^L \left[fN_i + \mu\frac{\partial f}{\partial x}\frac{\partial N_i}{\partial x}\right]\ dx \quad (22h)$$

4. Numerical results

Through this section, parametric studies are presented to illustrate effects of porosity models, porosity parameter, material gradation parameter, and nonlocal size-scale on the first five natural frequencies of FG porous nanobeam. Through this analysis, the constituent materials of the FG beam in the present study are steel metal and ceramic is alumina, whose properties are presented in Table 1. The thickness of FG porous nanobeam is 100 *nm*, however, the length and with are assumed to be 100 *h* and 10 *h*.

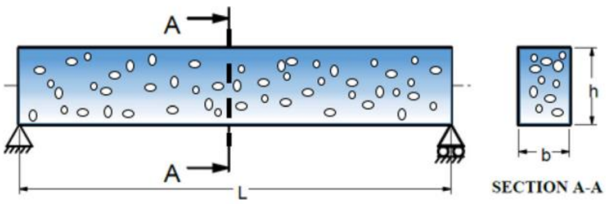

Fig. 4 Illustrate the geometrical dimension of simply-supported FG nanobeam structure , Eltaher *et al*. (2018b)

Table 1 Material properties of FGM constituents

Properties	Steel (metal)	Alumina (Al_2O_3) (ceramic)
E (GPa)	210	390
ρ (kg/m^3)	7800	3960
υ	0.3	0.3

In free vibration analysis, the eigenvalue problems are solved using the following relations

$$[K]\{\bar{d}\} = \omega^2[M]\{\bar{d}\} \quad (23)$$

where $\{\bar{d}\}$ represents the eigenvectors, λ are the eigenvalues (critical buckling loads), and ω^2 are the eigenvalues (natural frequencies) of the dynamic system. The nondimensional natural frequency is calculated according to the formula, $w_i = \omega_i^2 L^2 \sqrt{\frac{\rho_c A}{E_c I}}$.

4.1 Model validation

To validate this model, the nonlocal elasticity model is compared by results obtained by Reddy (2007), for isotropic material. As shown, the current results are identical as obtained by Redd (2007).

4.2 Effect of gradation parameter

The effect of gradation parameter on the first five natural frequencies of FG porous beam for different porosity models is presented in Figs. (5-9). As shown, by increasing gradation parameter the natural frequencies decreased sharply through a range of $0 \leq k \leq 2$. After that, approximately linear decreasing of the natural frequencies with a small rate is observed in case of $2 \leq k$, for all porosity model.

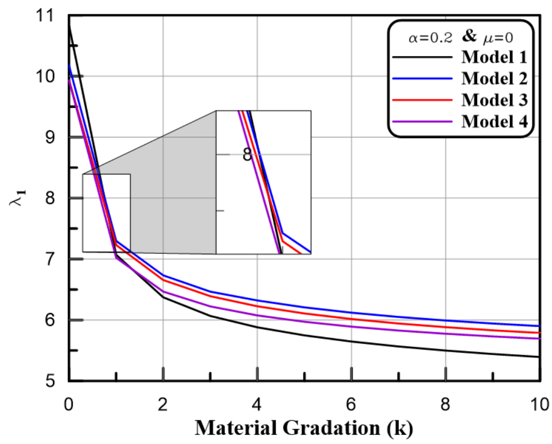

Fig. 5 Gradation Parameter Effect on the 1st natural frequencies for different porosity models at α=0.2 and μ=0

Table 2 The first natural frequency for isotopic material with different nonlocal parameter at L/h=10

μ	Reddy (2007)	Obtained Results
0	9.8696	9.8696
1	9.4159	9.4159
2	9.01495	9.0195
3	8.6693	8.6693
4	8.3569	8.3569

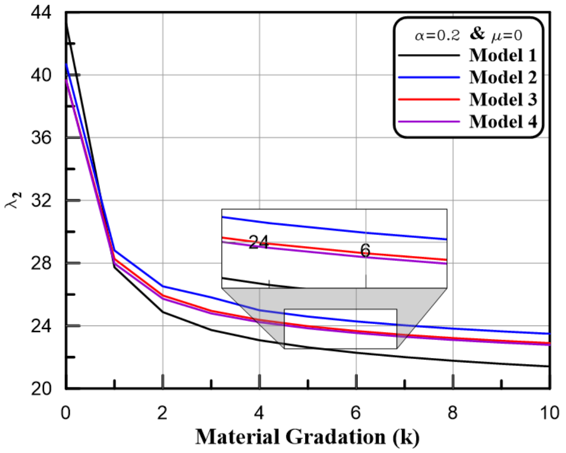

Fig. 6 Gradation Parameter Effect on the 2nd natural frequencies for different porosity models at α=0.2 and μ=0

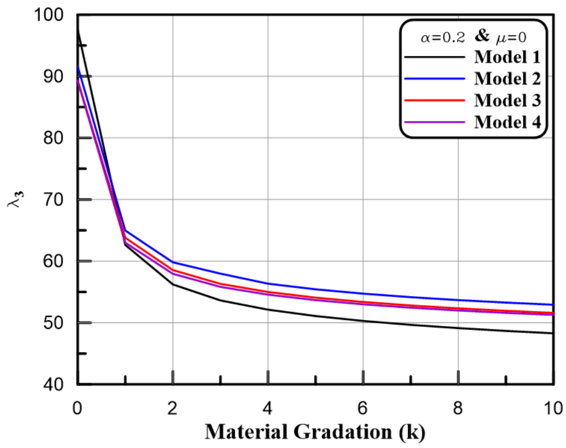

Fig. 7 Gradation Parameter Effect on the 3rd natural frequencies for different porosity models at α=0.2 and μ=0

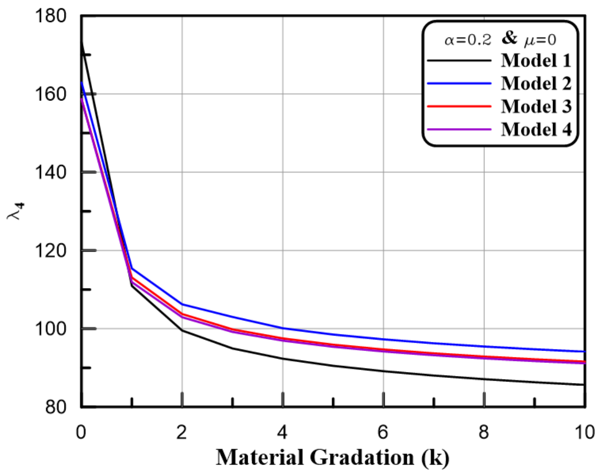

Fig. 8 Gradation Parameter Effect on the 4th natural frequencies for different porosity models at α=0.2 and μ=0

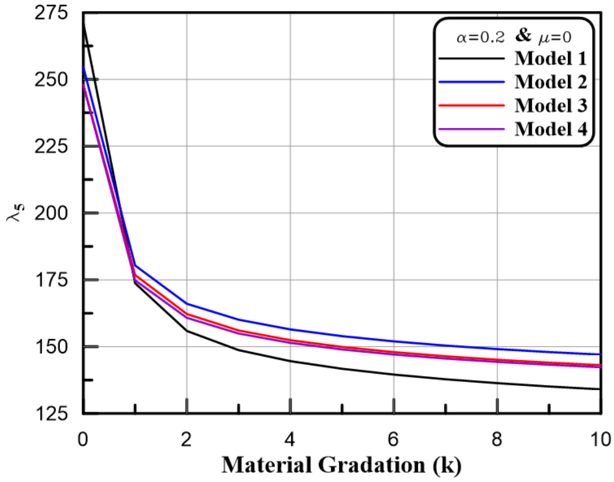

Fig. 9 Gradation Parameter Effect on the 5th natural frequencies for different porosity models at α=0.2 and μ=0

It is predicted from the figure that, natural frequencies for the first porosity model (uniform distribution) is the highest one in case of $k \leq 1$ and, it is the lowest frequencies in the range of $1 \leq k$. The natural frequency for porosity model 2 (symmetric distribution with mid-plane) is the highest one comparable by the other models if the gradation index greater than 1.

4.3 Effect of porosity parameter

The influence of porosity parameter on the first fife natural frequencies of FG porous nanobeam is illustrated in Figs. (10-14). At the beginning, all models have the same natural frequencies because the beam is fully without any porosity at $\alpha = 0$, and all models become the same. After that, there different phenomena. As shown porosity parameter has different effects on the frequencies of nanobeam according to the porosity model and mode number. As a case in hand, for the first natural frequency as depicted in Fig. 10, the neutral frequency decreased by increasing the porosity parameter for the uniform porosity distribution (Model 1). However, it has opposite effect in case of symmetric distribution through mid-plane, i.e., the 1^{st} natural frequency is increased proportionally with increasing the porosity parameter for model 2. For these two models, the porosity parameter has the same effect on the natural frequencies for the higher modes. In case of model 3, the first natural frequency is increased by increasing the porosity parameter. However, the higher frequencies are insignificant for the variation of porosity parameter. In case for, the first natural frequency decreases with increasing the porosity parameter and the higher frequencies remain constant by changing the porosity parameter. The highest natural frequencies are observed for model 2, and lowest natural frequencies are noticed for model 1. The natural frequencies for model 3 and model 4 are close to each other, as depicted in Figs. (11-14).

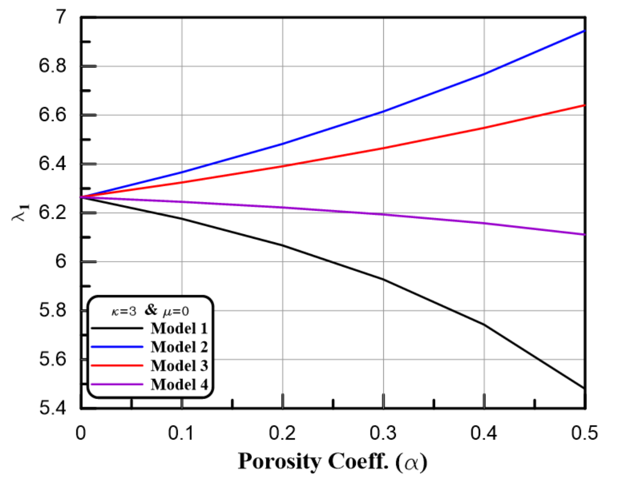

Fig. 10. Porosity parameter effect on the 1st natural frequencies for different porosity models at k=3.0 and μ=0

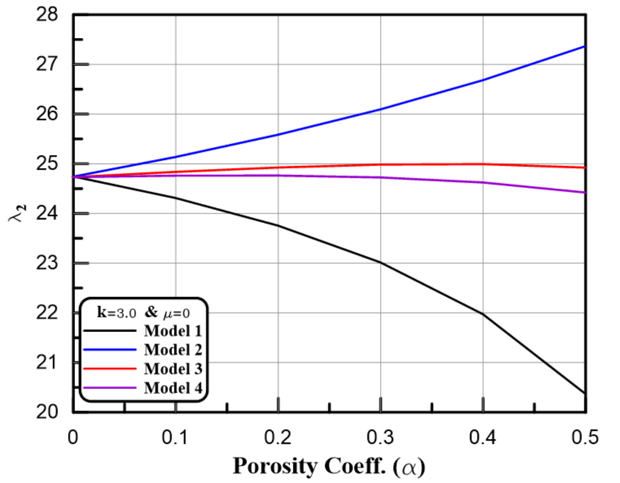

Fig. 11 Porosity parameter effect on the 2nd natural frequencies for different porosity models at k=3.0 and μ=0

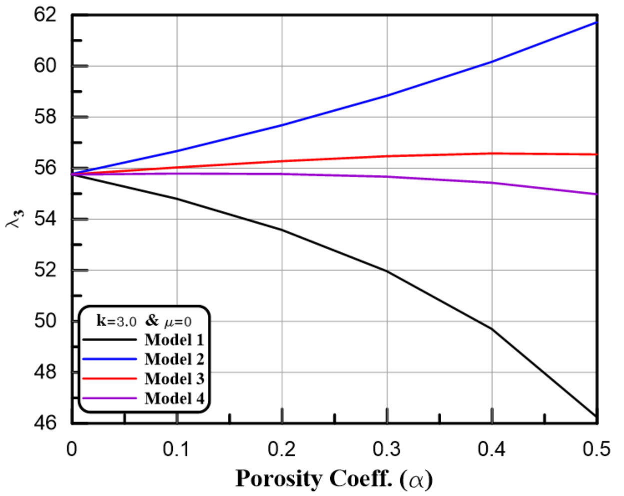

Fig. 12. Porosity parameter effect on the 3rd natural frequencies for different porosity models at k=3.0 and μ=0

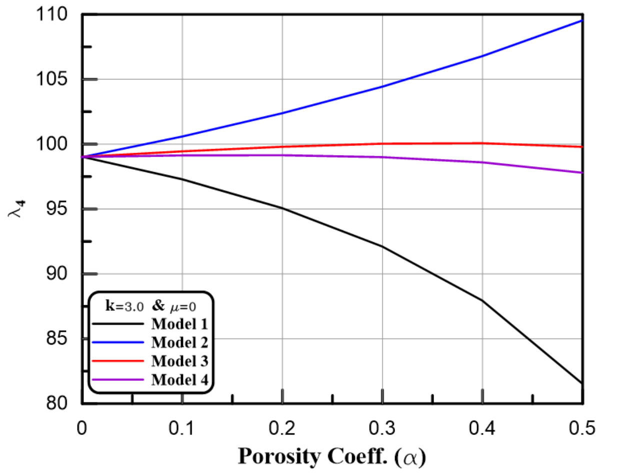

Fig. 13 Porosity parameter effect on the 4th natural frequencies for different porosity models at k=3.0 and μ=0

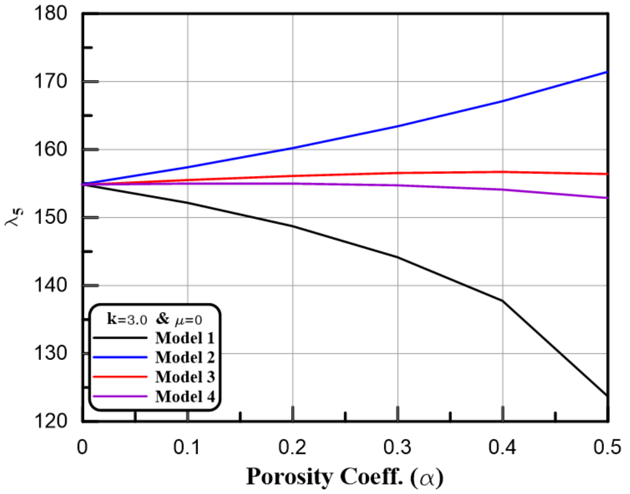

Fig. 14 Porosity parameter effect on the 5th natural frequencies for different porosity models at k=3.0 and μ=0

4.4 Nonlocal size-scale effect

The effects of nonlocal scale parameter on the 1st natural frequency of porous FG nanobeam for different gradation parameter as presented in Figs. (15-18). As shown in Fig. 11 for model 1, the effect of length scale is insignificant on the 1st natural frequency in the range of $k \leq 1$. By increasing the gradation parameter more than 1, the effect of nanoscale on the natural frequency becomes significant and tends to decrease the natural frequency by increasing its value. For other porosity models, shown in Figs. (16-18), by increasing the nonlocal parameter, the 1st natural frequency decreases gradually for any value of gradation parameter. It can conclude that, the nonlocal parameter tends to soften the material and thus decreasing its natural frequency.

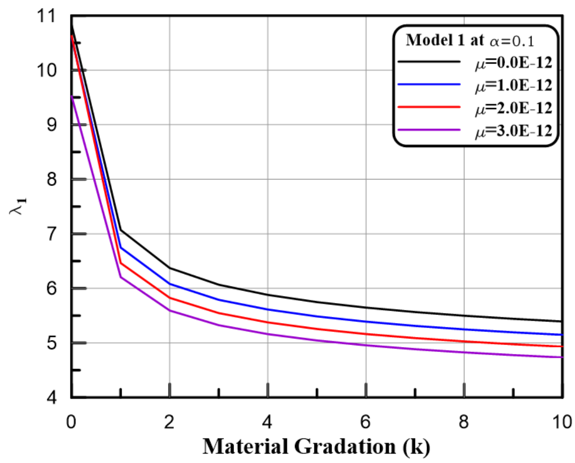

Fig. 15 Effect of nonlocal scale parameter on the 1st natural frequency of porous FG nanobeam α=0.2 for the porosity of model 1

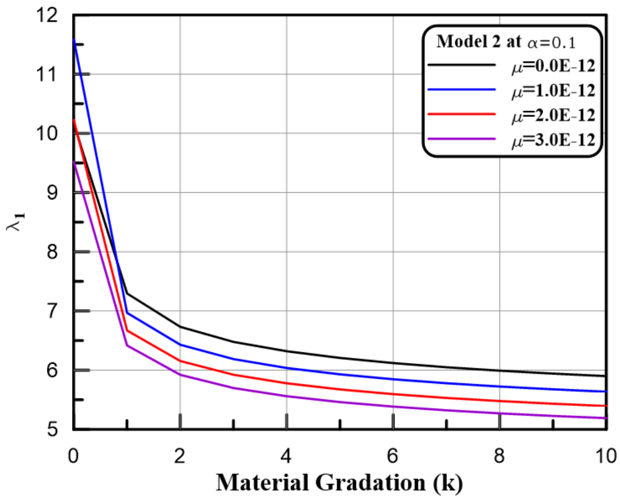

Fig. 16 Effect of nonlocal scale parameter on the 1st natural frequency of porous FG nanobeam α=0.2 for the porosity of model 2

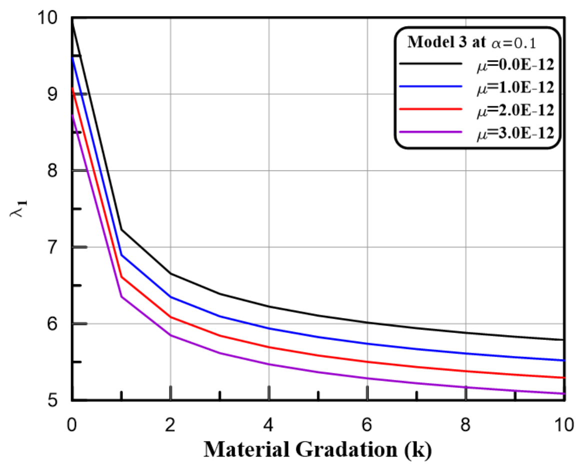

Fig. 17 Effect of nonlocal scale parameter on the 1st natural frequency of porous FG nanobeam α=0.2 for the porosity of model 3

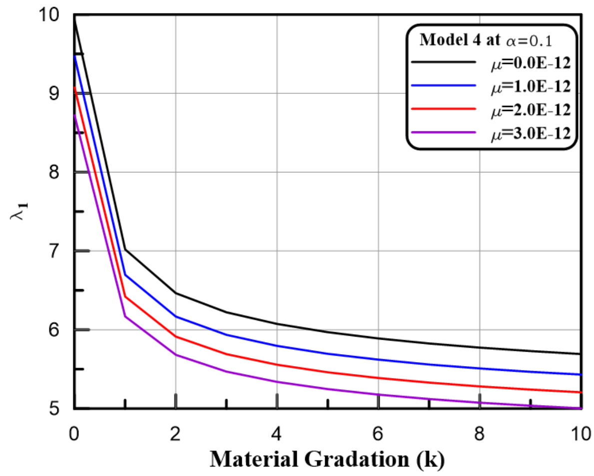

Fig. 18 Effect of nonlocal scale parameter on the 1st natural frequency of porous FG nanobeam α=0.2 for the porosity of model 4

5. Conclusions

In the framework of continuum mechanics, the free vibration of functional graded porous nanobeam is investigated. Different porosity models, such as uniform porosity distribution, symmetric with mid-plane, bottom surface distribution and top surface distribution, are proposed through analysis. Modified continuum model is adopted by include nano-scale effect by nonlocal Eringen theory. The mathematical model is solved numerically using the finite element method. The most findings of the current analysis can be summarized as: -.

- By increasing gradation parameter, the natural frequencies decreased sharply through a range of $0 \le k \le 2$. After that, approximately linear decreasing of the natural frequencies with a small rate is observed in case of $2 \le k$.
- Natural frequencies for the first porosity model (uniform distribution) is the highest one in case of $k \le 1$ and, it is the lowest frequencies in the range of $1 \le k$.
- The natural frequency for porosity model 2 (symmetric distribution with mid-plane) is the highest one comparable by the other models if the gradation index greater than 1
- Porosity parameter has different effects on the frequencies of nanobeam according to the porosity model and mode number.
- The nonlocal parameter tends to soften the material and thus decreasing its natural frequency.

Acknowledgments

This project was funded by the Deanship of Scientific Research (DSR), King Abdulaziz University, Jeddah, under grant No. (D-296-135-1440). The authors, therefore, gratefully acknowledge DSR technical and financial support.

References

Ahouel, M., Houari, M.S.A., Bedia, E.A. and Tounsi, A. (2016), "Size-dependent mechanical behavior of functionally graded trigonometric shear deformable nanobeams including neutral surface position concept", *Steel Compos. Struct.*, **20**(5), 963-981. https://doi.org/10.12989/scs.2016.20.5.963.

Agwa, M.A. and Eltaher, M.A. (2016), "Vibration of a carbyne nanomechanical mass sensor with surface effect", *Appl. Phys. A*, **122**(4), 335. https://doi.org/10.1007/s00339-016-9934-9.

Akbaş, Ş.D. (2015), "Free vibration and bending of functionally graded beams resting on elastic foundation", *Research on Engineering Structures and Materials*, **1**(1), 25-37. http://dx.doi.org/10.17515/resm2015.03st0107

Akbaş, Ş.D. (2017a), "Forced vibration analysis of functionally graded nanobeams", *Int. J. Appl. Mech.*, **9**(7), 1750100. https://doi.org/10.1142/S1758825117501009.

Akbaş, Ş.D. (2017b), "Thermal effects on the vibration of functionally graded deep beams with porosity", *Int. J. Appl. Mech.*, **9**(5), 1750076. https://doi.org/10.1142/S1758825117500764.

Akbaş, Ş.D. (2017c), "Nonlinear static analysis of functionally graded porous beams under thermal effect", *Coupled Syst. Mech.*, **6**(4), 399-415. https://doi.org/10.12989/csm.2017.6.4.399.

Akbaş, Ş.D. (2017d), "Vibration and static analysis of functionally graded porous plates", *J. Appl. Comput. Mech.*, **3**(3), 199-207. https://doi.org/10.22055/JACM.2017.21540.1107.

Akbas, S.D. (2018a), "Forced vibration analysis of cracked functionally graded microbeams", *Adv. Nano Res.*, **6**(1), 39. https://doi.org/10.12989/anr.2018.6.1.039.

Akbaş, Ş.D. (2018b), "Geometrically nonlinear analysis of functionally graded porous beams", *Wind Struct.*, **27**(1), 59-70. https://doi.org/10.12989/was.2018.27.1.059.

Akbaş, Ş.D. (2018c), "Forced vibration analysis of functionally graded porous deep beams", *Compos. Struct.*, **186**, 293-302. https://doi.org/10.1016/j.compstruct.2017.12.013

Akbaş, Ş.D. (2019a), "Longitudinal forced vibration analysis of porous a nanorod", *Mühendislik Bilimleri ve Tasarım Dergisi*, **7**(4), 736-743.

Akbaş, Ş.D. (2019b), "Forced vibration analysis of functionally graded sandwich deep beams", *Coupled Syst. Mech.*, **8**(3), 259-271. https://doi.org/10.12989/csm.2019.8.3.259.

Akbaş, Ş.D. (2019c), "Hygro-thermal post-buckling analysis of a functionally graded beam", *Coupled Syst. Mech.*, **8**(5), 459-471. https://doi.org/10.12989/csm.2019.8.5.459

Akbaş, Ş.D., Fageehi, Y.A., Assie, A.E. and Eltaher, M.A. (2020), "Dynamic analysis of viscoelastic functionally graded porous thick beams under pulse load", *Eng. with Comput.*, https://doi.org/10.1007/s00366-020-01070-3.

Almitani, K.H., Abdelrahman, A.A. and Eltaher, M.A. (2020), "Stability of perforated nanobeams incorporating surface energy effects", *Steel Compos. Struct.*, **35**(4), 555-566. https://doi.org/10.12989/scs.2020.35.4.555.

Alshorbagy, A.E., Eltaher, M.A. and Mahmoud, F.F. (2011), "Free vibration characteristics of a functionally graded beam by finite element method", *Appl. Math. Model.*, **35**(1), 412-425. https://doi:10.1016/j.apm.2010.07.006.

Amar, L.H.H., Kaci, A. and Tounsi, A. (2017), "On the size-dependent behavior of functionally graded micro-beams with porosities", *Struct. Eng. Mech.*, **64**(5), 527-541. https://doi.org/10.12989/sem.2017.64.5.527.

Apuzzo, A., Barretta, R., Luciano, R., de Sciarra, F.M. and Penna, R. (2017), "Free vibrations of Bernoulli-Euler nano-beams by the stress-driven nonlocal integral model", *Compos. Part B: Eng.*, **123**, 105-111. https://doi.org/10.1016/j.compositesb.2017.03.057.

Aria, A.I. and Friswell, M.I. (2019), "A nonlocal finite element model for buckling and vibration of functionally graded nanobeams", *Compos. Part B: Eng.*, **166**, 233-246. https://doi.org/10.1016/j.compositesb.2018.11.071.

Asiri, S.A., Akbas, S.D. and Eltaher, M.A. (2020), "Dynamic analysis of layered functionally graded viscoelastic deep beams with different boundary conditions due to a pulse load", *Int. J. Appl. Mech.*, https://doi.org/10.1142/S1758825120500556.

Bambaeechee, M. (2019), "Free vibration of AFG beams with elastic end restraints", *Steel Compos. Struct.*, **33**(3), 403-432. https://doi.org/10.12989/scs.2019.33.3.403.

Barretta, R., Čanadija, M., Feo, L., Luciano, R., de Sciarra, F.M., and Penna, R. (2018), "Exact solutions of inflected functionally graded nano-beams in integral elasticity", *Compos. Part B: Eng.*, **142**, 273-286. https://doi.org/10.1016/j.compositesb.2017.12.022.

Benahmed, A., Fahsi, B., Benzair, A., Zidour, M., Bourada, F. and Tounsi, A. (2019), "Critical buckling of functionally graded nanoscale beam with porosities using nonlocal higher-order shear deformation", *Struct. Eng. Mech.*, **69**(4), 457-466. https://doi.org/10.12989/sem.2019.69.4.457.

Berghouti, H., Adda Bedia, E.A., Benkhedda, A. and Tounsi, A. (2019), "Vibration analysis of nonlocal porous nanobeams made of functionally graded material", *Adv. Nano Res.*, **7**(5), 351-364. https://doi.org/10.12989/anr.2019.7.5.351.

Ebrahimi, F. and Habibi, S. (2016), "Deflection and vibration analysis of higher-order shear deformable compositionally graded porous plate", *Steel Compos. Struct.*, **20**(1), 205-225. https://doi.org/10.12989/scs.2016.20.1.205.

Eltaher, M.A., Emam, S.A. and Mahmoud, F.F. (2012), "Free vibration analysis of functionally graded size-dependent nanobeams", *Appl. Mathematics Comput.*, **218**(14), 7406-7420. https://doi.org/10.1016/j.amc.2011.12.090.

Eltaher, M.A., Emam, S.A. and Mahmoud, F.F. (2013a), "Static and stability analysis of nonlocal functionally graded nanobeams", *Compos. Struct.*, **96**, 82-88. https://doi.org/10.1016/j.compstruct.2012.09.030. .

Eltaher, M.A., Alshorbagy, A.E. and Mahmoud, F.F. (2013b), "Determination of neutral axis position and its effect on natural frequencies of functionally graded macro/nanobeams", *Compos. Struct.*, **99**, 193-201. https://doi.org/10.1016/j.compstruct.2012.11.039.

Eltaher, M.A., Alshorbagy, A.E. and Mahmoud, F.F. (2013c), "Vibration analysis of Euler–Bernoulli nanobeams by using finite element method", *Appl. Math. Model.*, **37**(7), 4787-4797. https://doi.org/10.1016/j.apm.2012.10.016.

Eltaher, M.A., Abdelrahman, A.A., Al-Nabawy, A., Khater, M. and Mansour, A. (2014a), "Vibration of nonlinear graduation of nano-Timoshenko beam considering the neutral axis position", *Appl. Math. Comput.*, **235**, 512-529. https://doi.org/10.1016/j.amc.2014.03.028.

Eltaher, M.A., Khairy, A., Sadoun, A.M. and Omar, F.A. (2014b), "Static and buckling analysis of functionally graded Timoshenko nanobeams", *Appl. Math. Comput.*, **229**, 283-295. https://doi.org/10.1016/j.amc.2013.12.072.

Eltaher, M.A. and Agwa, M.A. (2016), "Analysis of size-dependent mechanical properties of CNTs mass sensor using energy equivalent model", *Sensor. Actuat. A: Phys.*, **246**, 9-17. https://doi.org/10.1016/j.sna.2016.05.009.

Eltaher, M.A., Khater, M.E. and Emam, S.A. (2016a), "A review on nonlocal elastic models for bending, buckling, vibrations, and wave propagation of nanoscale beams", *Appl. Math. Model.*,

40(5-6), 4109-4128. ttps://doi.org/10.1016/j.apm.2015.11.026.
Eltaher, M.A., Khater, M.E., Park, S., Abdel-Rahman, E. and Yavuz, M. (2016b), "On the static stability of nonlocal nanobeams using higher-order beam theories", *Adv. Nano Res.*, **4**(1), 51. https://doi.org/10.12989/anr.2016.4.1.051.
Eltaher, M.A., El-Borgi, S. and Reddy, J.N. (2016c). "Nonlinear analysis of size-dependent and material-dependent nonlocal CNTs", *Compos. Struct.*, **153**, 902-913. https://doi.org/10.1016/j.compstruct.2016.07.013.
Eltaher, M.A., Attia, M.A., Soliman, A.E. and Alshorbagy, A.E. (2018a), "Analysis of crack occurs under unsteady pressure and temperature in a natural gas facility by applying FGM", *Struct. Eng. Mech.*, **66**(1), 97-111. https://doi.org/10.12989/sem.2018.66.1.097.
Eltaher, M.A., Fouda, N., El-midany, T. and Sadoun, A.M. (2018b), "Modified porosity model in analysis of functionally graded porous nanobeams", *J. Braz. Soc. Mech. Sci. Eng.*, **40**(3), 141. https://doi.org/10.1007/s40430-018-1065-0.
Eltaher, M.A., Kabeel, A.M., Almitani, K.H. and Abdraboh, A.M. (2018c), "Static bending and buckling of perforated nonlocal size-dependent nanobeams", *Microsystem Technologies*, **24**(12), 4881-4893. https://doi.org/10.1007/s00542-018-3905-3.
Eltaher, M.A., Abdraboh, A.M. and Almitani, K.H. (2018d), "Resonance frequencies of size dependent perforated nonlocal nanobeam", *Microsystem Technologies*, **24**(9), 3925-3937. https://doi.org/10.1007/s00542-018-3910-6.
Emam, S.A., Eltaher, M.A., Khater, M.E. and Abdalla, W.S. (2018), "Postbuckling and free vibration of multilayer imperfect nanobeams under a pre-stress load", *Appl. Sci.*, **8**(11), 2238. https://doi.org/10.3390/app8112238.
Eltaher, M.A., Omar, F.A., Abdalla, W.S. and Gad, E.H. (2019a), "Bending and vibrational behaviors of piezoelectric nonlocal nanobeam including surface elasticity", *Waves in Random and Complex Media*, **29**(2), 264-280. https://doi.org/10.1080/17455030.2018.1429693.
Eltaher, M.A., Almalki, T.A., Ahmed, K.I. and Almitani, K.H. (2019b), "Characterization and behaviors of single walled carbon nanotube by equivalent-continuum mechanics approach", *Adv. Nano Res.*, **7**(1), 39. https://doi.org/10.12989/anr.2019.7.1.039.
Eltaher, M.A. and Mohamed, N.A. (2020a), "Vibration of nonlocal perforated nanobeams with general boundary conditions", *Smart Struct. Syst.*, **25**(4), 501-514. https://doi.org/10.12989/sss.2020.25.4.501.
Eltaher, M.A. and Mohamed, N. (2020b), "Nonlinear stability and vibration of imperfect CNTs by Doublet mechanics", *Appl. Math. Comput.*, **382**, 125311. https://doi.org/10.1016/j.amc.2020.125311.
Eltaher, M.A. and Mohamed, S.A. (2020c), "Buckling and stability analysis of sandwich beams subjected to varying axial loads", *Steel Compos. Struct.*, **34**(2), 241-260. https://doi.org/10.12989/scs.2020.34.2.241.
Eringen, A.C. (1983), "On differential equations of nonlocal elasticity and solutions of screw dislocation and surface waves", *J. Appl. Phys.*, **54**(9), 4703-4710. https://doi.org/10.1063/1.332803.
Fenjan, R.M., Ahmed, R.A. and Faleh, N.M. (2020), "Nonlocal nonlinear dynamic behavior of composite piezo-magnetic beams using a refined higher-order beam theory", *Steel Compos. Struct.*, **35**(4), 545-554. https://doi.org/10.12989/scs.2020.35.4.545.
Gafour, Y., Hamidi, A., Benahmed, A., Zidour, M. and Bensattalah, T. (2020), "Porosity-dependent free vibration analysis of FG nanobeam using non-local shear deformation and energy principle", *Adv. Nano Res.*, **8**(1), 37-47. https://doi.org/10.12989/anr.2020.8.1.037.
Galeban, M.R., Mojahedin, A., Taghavi, Y. and Jabbari, M. (2016), "Free vibration of functionally graded thin beams made of saturated porous materials", *Steel Compos. Struct.*, **21**(5), 999-1016. https://doi.org/10.12989/scs.2016.21.5.999.
Guessas, H., Zidour, M., Meradjah, M. and Tounsi, A. (2018), "The critical buckling load of reinforced nanocomposite porous plates", *Struct. Eng. Mech.*, **67**(2), 115-123. https://doi.org/10.12989/sem.2018.67.2.115.
Gul, U. and Aydogdu, M. (2018), Noncoaxial vibration and buckling analysis of embedded double-walled carbon nanotubes by using doublet mechanics", *Compos. Part B: Eng.*, **137**, 60-73. https://doi.org/10.1016/j.compositesb.2017.11.005.
Hamed, M.A., Eltaher, M.A., Sadoun, A.M. and Almitani, K.H. (2016), "Free vibration of symmetric and sigmoid functionally graded nanobeams", *Appl. Phys. A*, **122**(9), 829. https://doi.org/10.1007/s00339-016-0324-0.
Hamed, M.A., Sadoun, A.M. and Eltaher, M.A. (2019), "Effects of porosity models on static behavior of size dependent functionally graded beam", *Struct. Eng. Mech.*, **71**(1), 89-98. https://doi.org/10.12989/sem.2019.71.1.089.
Hamed, M.A., Mohamed, S.A. and Eltaher, M.A. (2020a), "Buckling analysis of sandwich beam rested on elastic foundation and subjected to varying axial in-plane loads", *Steel Compos. Struct.*, **34**(1), 75-89. https://doi.org/10.12989/scs.2020.34.1.075.
Hamed M.A., Abu-bakr, R.M., Mohamed, S.A. and Eltaher, M.A. (2020b), "Influence of Axial Load Function and Optimization on Static Stability of Sandwich Functionally Graded Beams with Porous Core", *Eng. with Comput.*. https://doi.org/10.1007/s00366-020-01023-w.
Heydari, A. (2018), "Exact vibration and buckling analyses of arbitrary gradation of nano-higher order rectangular beam", *Steel Compos. Struct.*, **28**(5), 589-606. https://doi.org/10.12989/scs.2018.28.5.589 .
Jandaghian, A.A. and Rahmani, O. (2017), "Vibration analysis of FG nanobeams based on third-order shear deformation theory under various boundary conditions", *Steel Compos. Struct.*, **25**(1), 67-78. https://doi.org/10.12989/scs.2017.25.1.067.
Karami, B., Janghorban, M. and Rabczuk, T. (2020), "Dynamics of two-dimensional functionally graded tapered Timoshenko nanobeam in thermal environment using nonlocal strain gradient theory", *Compos. Part B: Eng.*, **182**, 107622. https://doi.org/10.1016/j.compositesb.2019.107622.
Khater, M.E., Eltaher, M.A., Abdel-Rahman, E. and Yavuz, M. (2014), "Surface and thermal load effects on the buckling of curved nanowires", *Eng. Sci. Technol. Int. J.*, **17**(4), 279-283. https://doi.org/10.1016/j.jestch.2014.07.003.
Khatir, S., Tiachacht, S., Thanh, C.L., Bui, T.Q. and Wahab, M.A. (2019), "Damage assessment in composite laminates using ANN-PSO-IGA and Cornwell indicator", *Compos. Struct.*, **230**, 111509. https://doi.org/10.1016/j.compstruct.2019.111509.
Kitipornchai, S., Chen, D. and Yang, J. (2017), "Free vibration and elastic buckling of functionally graded porous beams reinforced by graphene platelets", *Mater. Design*, **116**, 656-665. http://dx.doi.org/10.1016/j.matdes.2016.12.061.
Lee, J.C. and Ahn, S.H. (2018), "Bulk density measurement of porous functionally graded materials", *Int. J. Precision Eng. Manufact.*, **19**(1), 31-37. DOI: 10.1007/s12541-018-0004-4.
Liu, H., Lv, Z. and Wu, H. (2019), "Nonlinear free vibration of geometrically imperfect functionally graded sandwich nanobeams based on nonlocal strain gradient theory", *Compos. Struct.*, **214**, 47-61. https://doi.org/10.1016/j.compstruct.2019.01.090.
Matuła, I., Dercz, G. and Barczyk, J. (2019), "Titanium/Zirconium functionally graded materials with porosity gradients for potential biomedical applications", *Mater. Sci. Technol.*, 1-6. https://doi.org/10.1080/02670836.2019.1593603.
Mekerbi, M., Benyoucef, S., Mahmoudi, A., Bourada, F. and

Tounsi, A. (2019), "Investigation on thermal buckling of porous FG plate resting on elastic foundation via quasi 3D solution", *Struct. Eng. Mech.*, **72**(4), 513-524. https://doi.org/10.12989/sem.2019.72.4.513.

Melaibari, A., Khoshaim, A. B., Mohamed, S.A. and Eltaher, M. A. (2020), "Static stability and of symmetric and sigmoid functionally graded beam under variable axial load", *Steel Compos. Struct.*, **35**(5), 671-685. https://doi.org/10.12989/scs.2020.35.5.671.

Mirjavadi, S.S., Afshari, B.M., Shafiei, N., Hamouda, A.M.S. and Kazemi, M. (2017), "Thermal vibration of two-dimensional functionally graded (2D-FG) porous Timoshenko nanobeams", *Steel Compos. Struct.*, **25**(4), 415-426. https://doi.org/10.12989/scs.2017.25.4.415.

Miyamoto, Y., Kaysser, W.A., Rabin, B.H., Kawasaki, A. and Ford, R.G. (Eds.). (2013), "Functionally graded materials: design, processing and applications" (Vol. 5), *Springer Science & Business Media*.

Mirzaei, M.M.H., Loghman, A. and Arefi, M. (2019), "Time-dependent creep analysis of a functionally graded beam with trapezoidal cross section using first-order shear deformation theory", *Steel Compos. Struct.*, **30**(6), 567-576. https://doi.org/10.12989/scs.2019.30.6.567.

Mohamed, N., Mohamed, S.A. and Eltaher, M.A. (2020), "Buckling and post-buckling behaviors of higher order carbon nanotubes using energy-equivalent model", *Eng. with Comput.*, 1-14. https://doi.org/10.1007/s00366-020-00976-2.

Nguyen, D.K. and Tran, T.T. (2018), "Free vibration of tapered BFGM beams using an efficient shear deformable finite element model", *Steel Compos. Struct.*, **29**(3), 363-377. https://doi.org/10.12989/scs.2018.29.3.363.

Nguyen, H.X., Nguyen, T.N., Abdel-Wahab, M., Bordas, S.P., Nguyen-Xuan, H. and Vo, T.P. (2017), "A refined quasi-3D isogeometric analysis for functionally graded microplates based on the modified couple stress theory", *Comput. Method. Appl. M.*, **313**, 904-940. https://doi.org/10.1016/j.cma.2016.10.002.

Phung-Van, P., Ferreira, A.J.M., Nguyen-Xuan, H. and Wahab, M. A. (2017a), "An isogeometric approach for size-dependent geometrically nonlinear transient analysis of functionally graded nanoplates", *Compos. Part B: Eng.*, **118**, 125-134. https://doi.org/10.1016/j.compositesb.2017.03.012.

Phung-Van, P., Tran, L.V., Ferreira, A.J.M., Nguyen-Xuan, H. and Abdel-Wahab, M. (2017b), "Nonlinear transient isogeometric analysis of smart piezoelectric functionally graded material plates based on generalized shear deformation theory under thermo-electro-mechanical loads", *Nonlinear Dynam.*, **87**(2), 879-894. https://doi.org/10.1007/s11071-016-3085-6.

Phung-Van, P., Thanh, C.L., Nguyen-Xuan, H. and Abdel-Wahab, M. (2018), "Nonlinear transient isogeometric analysis of FG-CNTRC nanoplates in thermal environments", *Compos. Struct.*, **201**, 882-892. https://doi.org/10.1016/j.compstruct.2018.06.087.

Phung-Van, P., Thai, C.H., Nguyen-Xuan, H. and Wahab, M.A. (2019), "Porosity-dependent nonlinear transient responses of functionally graded nanoplates using isogeometric analysis", *Compos. Part B: Eng.*, **164**, 215-225. https://doi.org/10.1016/j.compositesb.2018.11.036.

Rahmani, O. and Pedram, O. (2014), "Analysis and modeling the size effect on vibration of functionally graded nanobeams based on nonlocal Timoshenko beam theory", *Int. J. Eng. Sci.*, **77**, 55-70. https://doi.org/10.1016/j.ijengsci.2013.12.003.

Rahmani, O., Hosseini, S.A.H., Ghoytasi, I. and Golmohammadi, H. (2018), "Free vibration of deep curved FG nano-beam based on modified couple stress theory", *Steel Compos. Struct.*, **26**(5), 607-20. https://doi.org/10.12989/scs.2018.26.5.607.

Reddy, J.N. (2007), "Nonlocal theories for bending, buckling and vibration of beams", *Int. J. Eng. Sci.*, **45**(2-8), 288-307. https://doi.org/10.1016/j.ijengsci.2007.04.004.

Reddy, J.N. (2011), "Microstructure-dependent couple stress theories of functionally graded beams", *J. Mech. Phys. Solids*, **59**(11), 2382-2399. https://doi.org/10.1016/j.jmps.2011.06.008.

Shaat, M., Eltaher, M.A., Gad, A.I. and Mahmoud, F.F. (2013), "Nonlinear size-dependent finite element analysis of functionally graded elastic tiny-bodies", *Int. J. Mech. Sci.*, **77**, 356-364. https://doi.org/10.1016/j.ijmecsci.2013.04.015.

Şimşek, M. and Yurtcu, H.H. (2013), "Analytical solutions for bending and buckling of functionally graded nanobeams based on the nonlocal Timoshenko beam theory", *Compos. Struct.*, **97**, 378-386. https://doi.org/10.1016/j.compstruct.2012.10.038.

Şimşek, M. (2016), "Nonlinear free vibration of a functionally graded nanobeam using nonlocal strain gradient theory and a novel Hamiltonian approach", *Int. J. Eng. Sci.*, **105**, 12-27. https://doi.org/10.1016/j.ijengsci.2016.04.013.

Şimşek, M. (2019), "Some closed-form solutions for static, buckling, free and forced vibration of functionally graded (FG) nanobeams using nonlocal strain gradient theory", *Compos. Struct.*, **224**, 111041. https://doi.org/10.1016/j.compstruct.2019.111041.

Soliman, A.E., Eltaher, M.A., Attia, M.A. and Alshorbagy, A.E. (2018), "Nonlinear transient analysis of FG pipe subjected to internal pressure and unsteady temperature in a natural gas facility", *Struct. Eng. Mech.*, **66**(1), 85-96. https://doi.org/10.12989/sem.2018.66.1.085.

Thai, H.T. (2012), "A nonlocal beam theory for bending, buckling, and vibration of nanobeams", *Int. J. Eng. Sci.*, **52**, 56-64. https://doi.org/10.1016/j.ijengsci.2011.11.011.

Thang, P.T., Nguyen-Thoi, T., Lee, D., Kang, J. and Lee, J. (2018), "Elastic buckling and free vibration analyses of porous-cellular plates with uniform and non-uniform porosity distributions", *Aerosp. Sci. Technol.*, **79**, 278-287. https://doi.org/10.1016/j.ast.2018.06.010.

Thanh, C.L., Phung-Van, P., Thai, C.H., Nguyen-Xuan, H. and Wahab, M.A. (2018), "Isogeometric analysis of functionally graded carbon nanotube reinforced composite nanoplates using modified couple stress theory", *Compos. Struct.*, **184**, 633-649. https://doi.org/10.1016/j.compstruct.2017.10.025.

Thanh, C.L., Ferreira, A.J.M. and Wahab, M.A. (2019a), "A refined size-dependent couple stress theory for laminated composite micro-plates using isogeometric analysis", *Thin-Wall. Struct.*, **145**, 106427. https://doi.org/10.1016/j.tws.2019.106427.

Thanh, C.L., Tran, L.V., Vu-Huu, T. and Abdel-Wahab, M. (2019b), "The size-dependent thermal bending and buckling analyses of composite laminate microplate based on new modified couple stress theory and isogeometric analysis", *Comput. Method. Appl. M.*, **350**, 337-361. https://doi.org/10.1016/j.cma.2019.02.028.

Thanh, C.L., Tran, L.V., Vu-Huu, T., Nguyen-Xuan, H. and Abdel-Wahab, M. (2019c), "Size-dependent nonlinear analysis and damping responses of FG-CNTRC micro-plates", *Comput. Method. Appl. M.*, **353**, 253-276. https://doi.org/10.1016/j.cma.2019.05.002.

Thanh, C.L., Tran, L.V., Bui, T.Q., Nguyen, H.X. and Abdel-Wahab, M. (2019d), "Isogeometric analysis for size-dependent nonlinear thermal stability of porous FG microplates", *Compos. Struct.*, **221**, 110838. https://doi.org/10.1016/j.compstruct.2019.04.010.

Trabelssi, M., El-Borgi, S., Ke, L. L., & Reddy, J. N. (2017), "Nonlocal free vibration of graded nanobeams resting on a nonlinear elastic foundation using DQM and LaDQM", *Compos. Struct.*, **176**, 736-747. https://doi.org/10.1016/j.compstruct.2017.06.010.

Wang, Y.Q., Wan, Y.H. and Zhang, Y.F. (2017), "Vibrations of longitudinally traveling functionally graded material plates with porosities", *Eur. J. Mech.-A/Solids*, **66**, 55-68. http://dx.doi.org/10.1016/j.euromechsol.2017.06.006.

Wattanasakulpong, N. and Ungbhakorn, V. (2014), "Linear and nonlinear vibration analysis of elastically restrained ends FGM beams with porosities", *Aerosp. Sci. Technol.*, **32**(1), 111-120. https://doi.org/10.1016/j.ast.2013.12.002.

Yahia, S.A., Atmane, H.A., Houari, M.S.A. and Tounsi, A. (2015), "Wave propagation in functionally graded plates with porosities using various higher-order shear deformation plate theories", *Struct. Eng. Mech.*, 53(6), 1143-1165. https://doi.org/10.12989/sem.2015.53.6.1143.

Yousfi, M., Atmane, H.A., Meradjah, M., Tounsi, A. and Bennai, R. (2018), "Free vibration of FGM plates with porosity by a shear deformation theory with four variables", *Struct. Eng. Mech.*, **66**(3), 353-368. https://doi.org/10.12989/sem.2018.66.3.353.

Yuksel, Y.Z. and Akbaş, Ş.D. (2019), "Buckling analysis of a fiber reinforced laminated composite plate with porosity", *J. Comput. Appl. Mech.*, **50**(2), 375-380. 10.22059/JCAMECH.2019.291967.448.

Zhang, Y. and Wang, J. (2017), "Fabrication of functionally graded porous polymer structures using thermal bonding lamination techniques", *Procedia Manufact.*, **10**, 866-875. https://doi.org/10.1016/j.promfg.2017.07.073.

Zhao, X., Zheng, S. and Li, Z. (2020), "Effects of porosity and flexoelectricity on static bending and free vibration of AFG piezoelectric nanobeams", *Thin-Wall. Struct.*, **151**, 106754. https://doi.org/10.1016/j.tws.2020.106754.

CC